AD-A090 111 FEDERAL AVIATION ADMINISTRATION TECHNICAL CENTER ATL--ETC F/G 17/9
TEST AND EVALUATION OF THE AIRPORT SURVEILLANCE RADAR (ASR)-8 W--ETC(U)
AUG 80 D L OFFI, W LEWIS, T LEE, A DELAMARCHE
UNCLASSIFIED FAA-CT-80-17-A FAA-RD-80-21-A NL

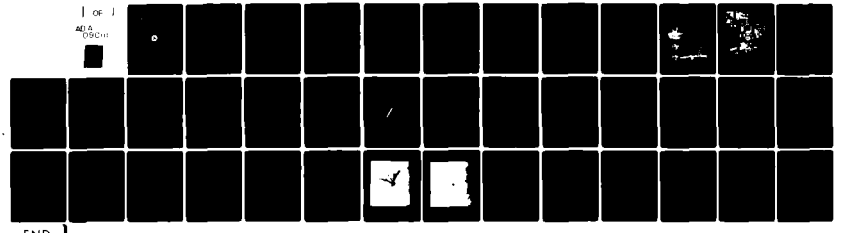

END
DATE FILMED
11-80
DTIC

Report No. FAA-RD-80-21A
FAA-CT-80-17A

TEST AND EVALUATION OF THE AIRPORT SURVEILLANCE RADAR (ASR)-8 WIND SHEAR DETECTION SYSTEM (PHASE II)

D. L. Offi - W. Lewis
T. Lee - A. DeLaMarche

FEDERAL AVIATION ADMINISTRATION TECHNICAL CENTER
Atlantic City, N. J. 08405

INTERIM REPORT
REVISED

AUGUST 1980

Prepared for

U. S. DEPARTMENT OF TRANSPORTATION
FEDERAL AVIATION ADMINISTRATION
Systems Research & Development Service
Washington, D. C. 20590

NOTICE

This document is disseminated under the sponsorship of the Department of Transportation in the interest of information exchange. The United States Government assumes no liability for the contents or use thereof.

The United States Government does not endorse products or manufacturers. Trade or manufacturer's names appear herein solely because they are considered essential to the object of this report.

Technical Report Documentation Page

1. Report No.	2. Government Accession No.	3. Recipient's Catalog No.
FAA-RD-80-21-A	AD-A090 111	

4. Title and Subtitle
TEST AND EVALUATION OF THE AIRPORT SURVEILLANCE RADAR (ASR)-8 WIND SHEAR DETECTION SYSTEM (PHASE II). Revision.

5. Report Date
August 1980

6. Performing Organization Code

7. Author(s)
D. L. Offi, W. Lewis, T. Lee, and A. DeLaMarche

8. Performing Organization Report No.
FAA-CT-80-17-A

9. Performing Organization Name and Address
Federal Aviation Administration
Technical Center
Atlantic City, New Jersey 08405

10. Work Unit No. (TRAIS)

11. Contract or Grant No.
022-242-830

12. Sponsoring Agency Name and Address
U.S. Department of Transportation
Federal Aviation Administration
Systems Research and Development Service
Washington, D.C. 20590

13. Type of Report and Period Covered
Interim rpt
April - December 1979

14. Sponsoring Agency Code

15. Supplementary Notes
This report revises and replaces original report, FAA-RD-80-21, dated May 1980.

16. Abstract

A wind shear detection system developed by the Wave Propagation Laboratory (WPL) to operate with the Federal Aviation Administration (FAA), Airport Surveillance Radar (ASR)-8 was installed and is being tested at the FAA Technical Center. Initial efforts, previously reported in Report NA-78-59-LR, were directed toward hardware and software shakedown and feasibility determination. Second phase tests compared radar with aircraft and tower winds, evaluated the wind shear measurement capability under various weather conditions, and investigated the effectiveness of a simple two-azimuth pointing strategy and system capabilities and limitations.

Results showed the system to be compatible with and to operate satisfactorily with the ASR-8. The processing and spectral display of clear air and precipitation returns is feasible. The accuracy of agreement between radar-measured winds and components of the aircraft-measured winds in both radially oriented flights and runway offset flights, using a two-azimuth pointing technique, was examined. Radar versus tower wind agreement was also examined. Potentially dangerous wind shears associated with weather during these tests were detectable. Certain system limitations also have been defined and considered. It is recommended that tests continue to complete definition of and demonstrate capabilities in all weather situations, to optimize performance, and to provide information to specify system design for possible development of a prototype model.

17. Key Words	18. Distribution Statement
Wind Wind Shear Doppler Radar Terminal Radar	Document is available to the U.S. public through the National Technical Information Service, Springfield, Virginia 22161

19. Security Classif. (of this report)	20. Security Classif. (of this page)	21. No. of Pages	22. Price
Unclassified	Unclassified	51	

Form DOT F 1700.7 (8-72) Reproduction of completed page authorized

411863

METRIC CONVERSION FACTORS

Approximate Conversions to Metric Measures

Symbol	When You Know	Multiply by	To Find	Symbol
	LENGTH			
in	inches	*2.5	centimeters	cm
ft	feet	30	centimeters	cm
yd	yards	0.9	meters	m
mi	miles	1.6	kilometers	km
	AREA			
in^2	square inches	6.5	square centimeters	cm^2
ft^2	square feet	0.09	square meters	m^2
yd^2	square yards	0.8	square meters	m^2
mi^2	square miles	2.6	square kilometers	km^2
	acres	0.4	hectares	ha
	MASS (weight)			
oz	ounces	28	grams	g
lb	pounds	0.45	kilograms	kg
	short tons (2000 lb)	0.9	tonnes	t
	VOLUME			
tsp	teaspoons	5	milliliters	ml
Tbsp	tablespoons	15	milliliters	ml
fl oz	fluid ounces	30	milliliters	ml
c	cups	0.24	liters	l
pt	pints	0.47	liters	l
qt	quarts	0.95	liters	l
gal	gallons	3.8	liters	l
ft^3	cubic feet	0.03	cubic meters	m^3
yd^3	cubic yards	0.76	cubic meters	m^3
	TEMPERATURE (exact)			
°F	Fahrenheit temperature	5/9 (after subtracting 32)	Celsius temperature	°C

* 1 in = 2.54 exactly. For other exact conversions and more detail tables, see NBS Misc. Publ. 286, Units of Weights and Measures, Price $2.25, SD Catalog No. C13.10:286.

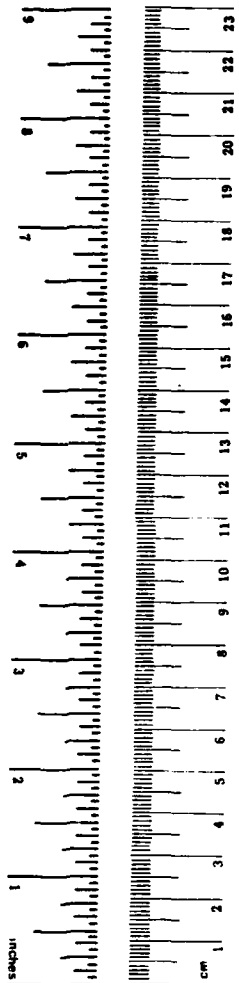

Approximate Conversions from Metric Measures

Symbol	When You Know	Multiply by	To Find	Symbol
	LENGTH			
mm	millimeters	0.04	inches	in
cm	centimeters	0.4	inches	in
m	meters	3.3	feet	ft
m	meters	1.1	yards	yd
km	kilometers	0.6	miles	mi
	AREA			
cm^2	square centimeters	0.16	square inches	in^2
m^2	square meters	1.2	square yards	yd^2
km^2	square kilometers	0.4	square miles	mi^2
ha	hectares (10,000 m^2)	2.5	acres	
	MASS (weight)			
g	grams	0.035	ounces	oz
kg	kilograms	2.2	pounds	lb
t	tonnes (1000 kg)	1.1	short tons	
	VOLUME			
ml	milliliters	0.03	fluid ounces	fl oz
l	liters	2.1	pints	pt
l	liters	1.06	quarts	qt
l	liters	0.26	gallons	gal
m^3	cubic meters	35	cubic feet	ft^3
m^3	cubic meters	1.3	cubic yards	yd^3
	TEMPERATURE (exact)			
°C	Celsius temperature	9/5 (then add 32)	Fahrenheit temperature	°F

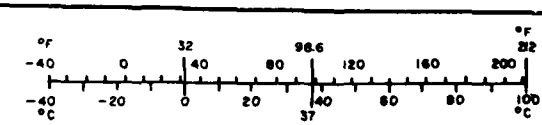

TABLE OF CONTENTS

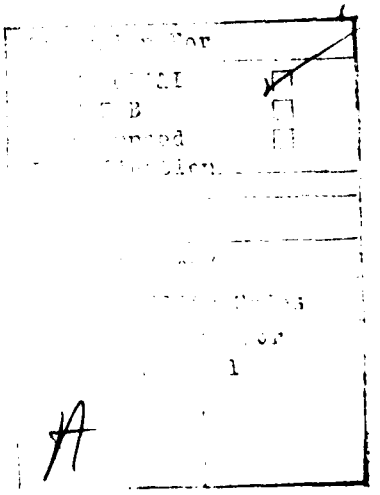

LIST OF ILLUSTRATIONS

LIST OF TABLES

INTRODUCTION

PURPOSE.

The purpose of this project is to determine the feasibility of using existing Federal Aviation Administration (FAA) terminal radars in conjunction with a new supplementary antenna and Fast Fourier Transform (FFT) data processing for the detection of hazardous low-level wind shear conditions in the optically clear atmosphere as well as in precipitation.

BACKGROUND.

Analyses of aircraft accidents have indicated that low-level wind shear has been the cause of nine terminal area accidents since 1972. Wind shear (abrupt change in wind direction and/or speed) increases or decreases the effective airflow over an aircraft's wings, causing it to go above or below its intended flightpath. This is especially dangerous during critical landing and takeoff maneuvers which leave little margin for corrective action.

Significant wind shear, the dimensions of which can be tens of miles in width, up to 200 miles in length, and hundreds of feet in vertical extent, occurs rather infrequently (in the order of 100 to 200 hours per year at the major air terminals). The meteorological mechanisms responsible for wind shear include the thunderstorm downdraft and gust front, frontal zones, and low-level jet streams. These hazardous phenomena can occur year round, and in the case of thunderstorm downdrafts and gustfronts, may be detected only after the fact by ground instrumentation or through pilot reports.

Under the sponsorship of the FAA Systems Research and Development Service (SRDS), Wind Shear and Wake Vortex Section, ARD-414, various solutions to the problem are being investigated. One possible solution being pursued by the Radar Section, ARD-231, is the use of specially instrumented terminal radars. In support of this effort, the Wave Propagation Laboratory (WPL) of the National Oceanic and Atmospheric Administration (NOAA), under Task VII of Interagency Agreement DOT-FA76 WAI-622, conducted appropriate analyses and design efforts for a system currently under evaluation at the FAA Technical Center.

Preliminary tests have been completed and previously reported (reference 1). This report describes efforts performed during the second phase of the test and evaluation.

SYSTEM DESCRIPTION.

The system configuration is illustrated in figure 1. The Airport Surveillance Radar (ASR)-8 is one channel of the standard dual-channel radar installed in the Center's Terminal Facility for Automated System Testing (TFAST). The parabolic 15-foot diameter antenna was installed on the roof of the building adjoining the radar and interconnected through a waveguide switching arrangement which allowed the radar to operate with either its standard search antenna or the wind shear antenna. The unmodified second channel was operated in an air traffic control (ATC) mode at all times. The remainder of the equipment, interconnected as shown in figure 1, is part of the WPL-developed system. Figures 2 and 3 are photographs of the antennas and equipment. Installation of the wind shear system did not require any modification of the ASR-8 other than rearrangement of the antenna transmission lines.

Referring to figure 1, the inphase and quadrature (I&Q) phase detector outputs are digitized. The resulting 10-bit words are stored in two, 64-word buffers which are transferred to the computer as 16-bit digital I&Q video. A 128-point FFT program is used to extract the Doppler information from the radar

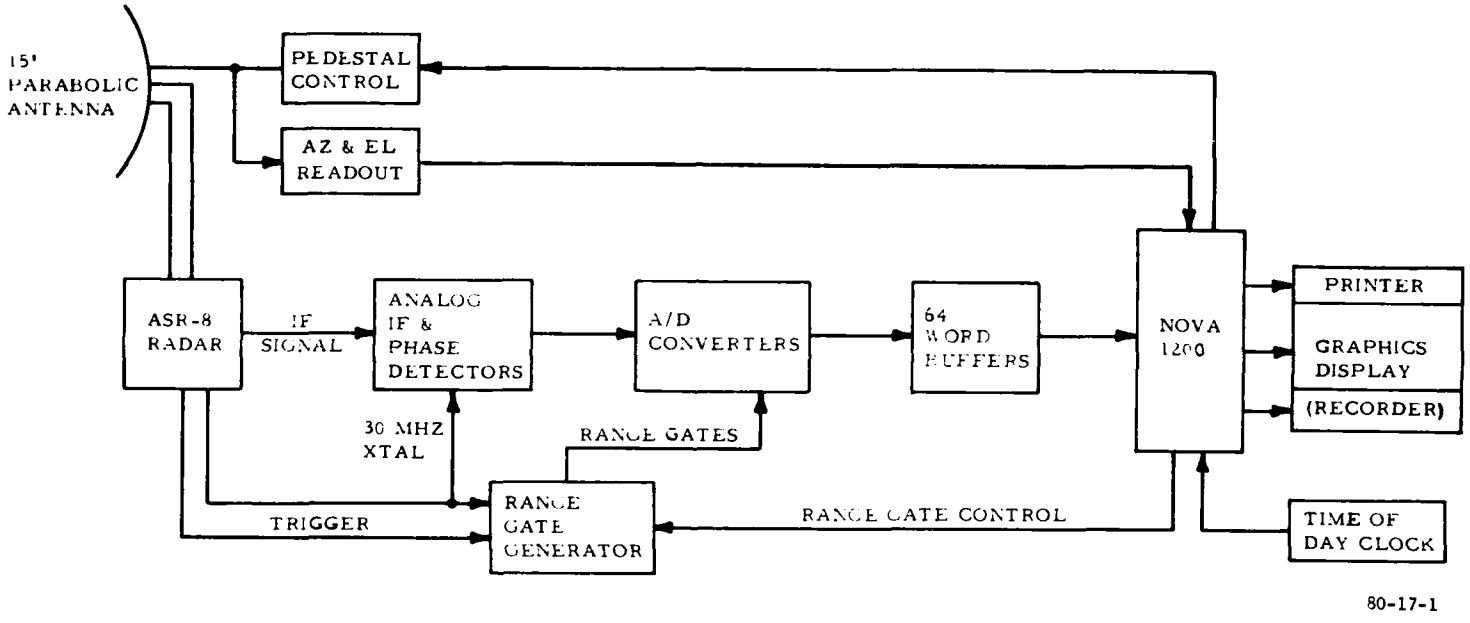

FIGURE 1. ASR-8 WIND SHEAR DETECTION SYSTEM

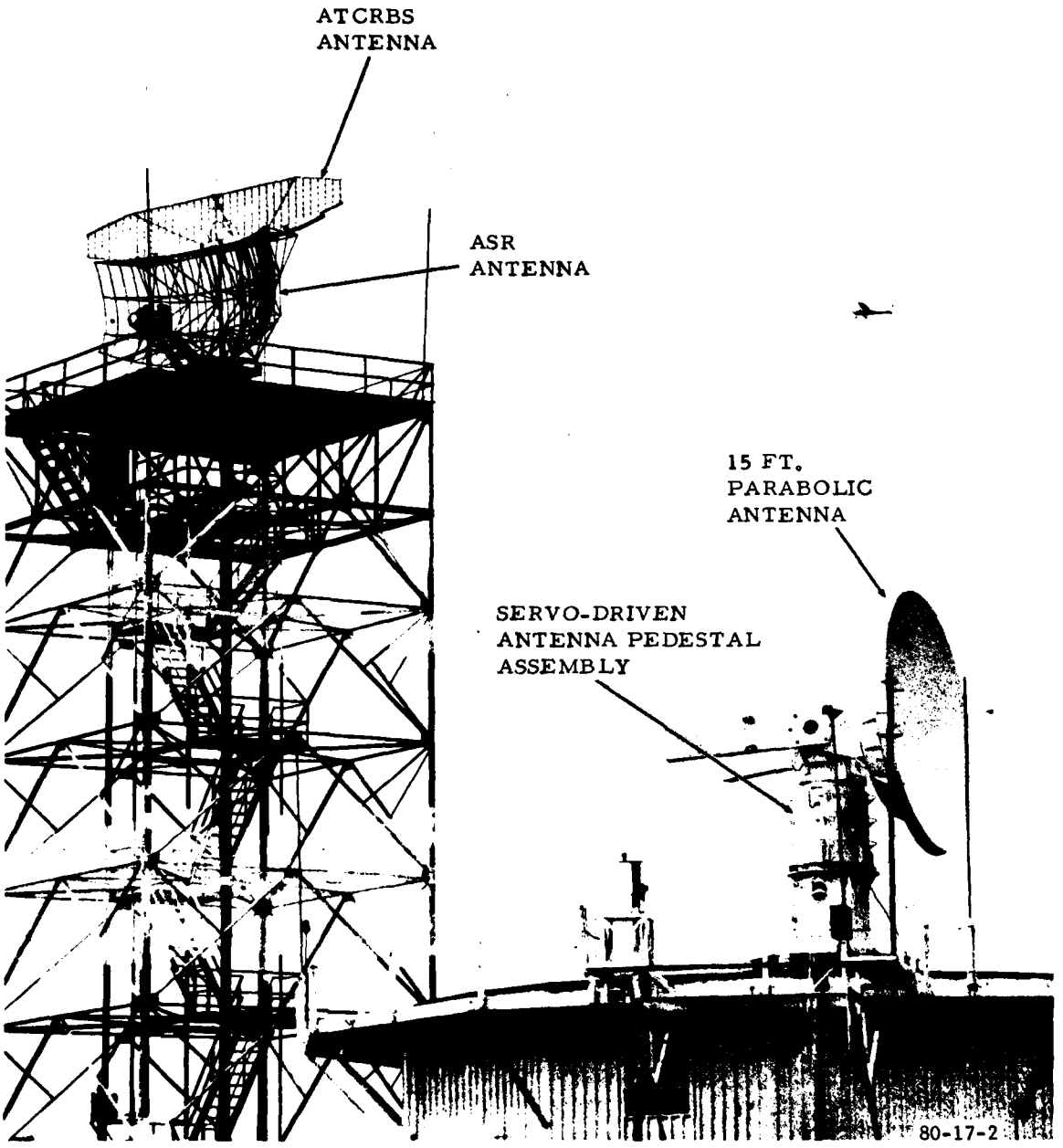

FIGURE 2. ASR AIR TRAFFIC CONTROL AND WIND SHEAR ANTENNAS

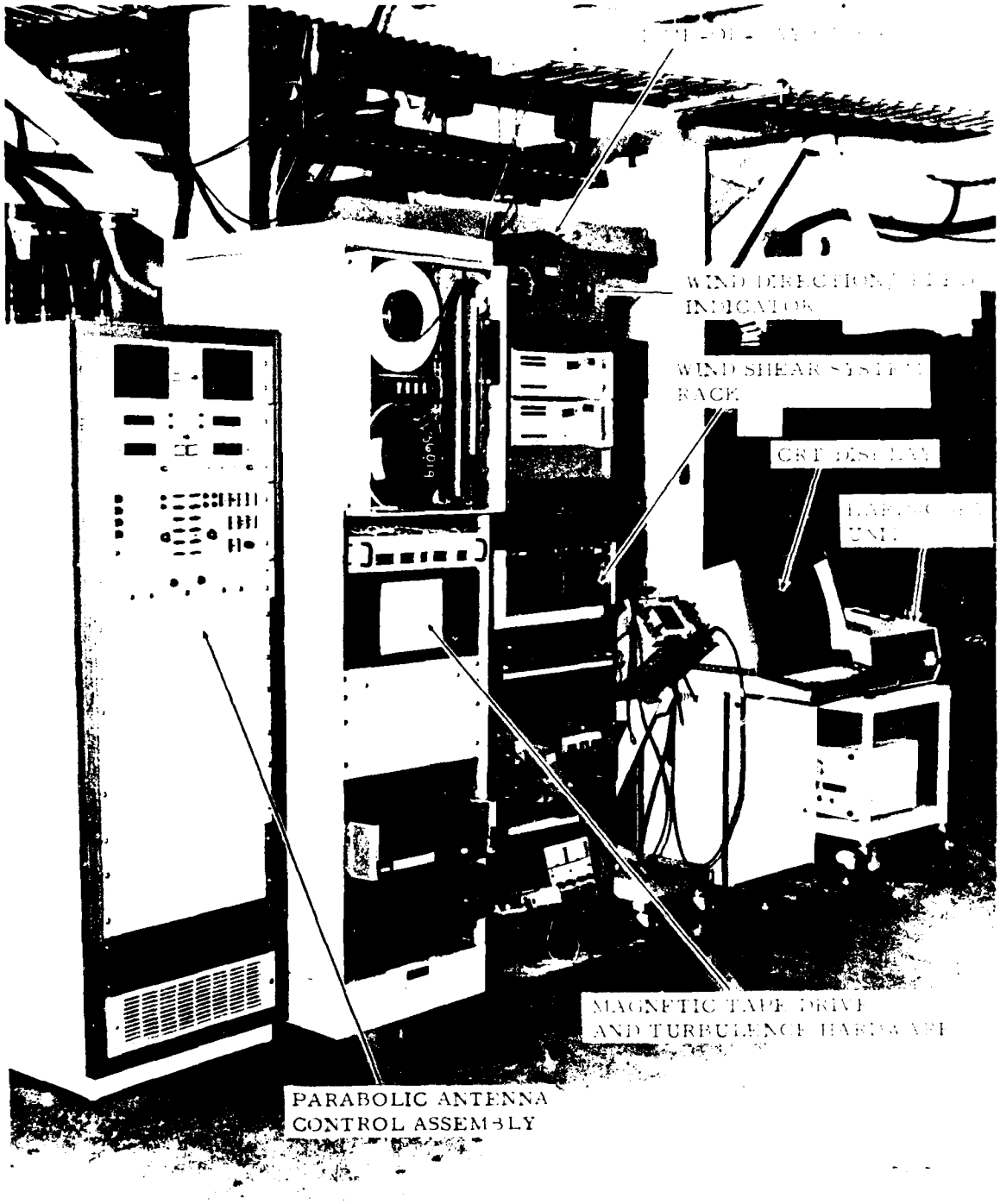

FIGURE 3. WIND SHEAR TEST BED EQUIPMENT LAYOUT

signals. The program outputs one range gate at the selected location, acquires data, calculates the power spectrum, repeats data acquisition and calculation, averages spectra, outputs spectra to display, then steps to the next range location. After calculating and displaying spectra for each range location, the sequence is repeated and new data replaces old data on the display. In addition, the data may be recorded on the diskette-type recorder for later playback and off-line processing. Additional programs include diagnostics for troubleshooting and testing and for data reduction and analysis routines.

DISCUSSION

PRELIMINARY TESTS.

Preliminary tests were conducted with the parabolic antenna mounted on a temporary fixed pedestal. This configuration provided very limited position adjustment capability. Tests were performed to determine feasibility and to check hardware and software.

Results (reference 1) showed the system to be compatible with the Technical Center ASR-8, and showed that the processing and spectral display of both clear-air and precipitation returns is feasible. Good agreement was experienced between radar-measured and aircraft-measured wind components in the pointing direction of the radar. Figure 4 is an example of the radar/aircraft data comparison.

SECOND PHASE TEST AND EVALUATION

The second phase of the project began after the installation of a new antenna drive pedestal assembly, as shown in figure 2. The pedestal allows positioning of the antenna from a remote control panel and from signals provided by the computer. The assembly was procured by the FAA according to a set of rigid performance specifications.

A new display was also obtained which includes a peripheral hard-copy unit that facilitates data reduction and analysis. Figures 5 and 6 are examples of spectral data from both precipitation and clear-air returns. Wind velocity, spectral width, intensity, scaling, and threshold level information are shown in the left portion of the display. The approximate range and elevation of each measurement sample are also shown. The remainder of this section concerns further radar/aircraft wind comparisons, radar/tower wind comparisons, and the results of measuring winds and terminal-area wind shears under various weather conditions at the Technical Center. Also included is the effectiveness of antenna pointing strategies in determining the wind along the glide slope, assuming horizontally uniform wind conditions, and the definition of system limitations and capabilities.

RADAR/AIRCRAFT WIND COMPARISON. Radar wind data were compared with aircraft wind data obtained with an inertial navigation system (INS)-equipped Center Gulfstream aircraft. The radar measurements were made in the clear air over a volume of space determined by the radar beam width (approximately 1.6° conical) and range resolution (pulse length of 90 meters). Observation time was about 1 second. The radar wind components were extracted manually from the type of data shown in figure 6 since the automatic program was not functioning. Occasionally, the wind signal was obscured by spurious signals or ground clutter. The aircraft measurements made along the track of the aircraft were averaged over a 5-second period and updated every 1.5 seconds. Both systems have an approximate $\pm$1-knot measurement accuracy.

Two operating procedures, simulated and actual, were used: (1) The aircraft flew simulated 3° glide slope approaches directly toward the radar site (assumed to be at the touchdown point) on a heading approximately aligned with the

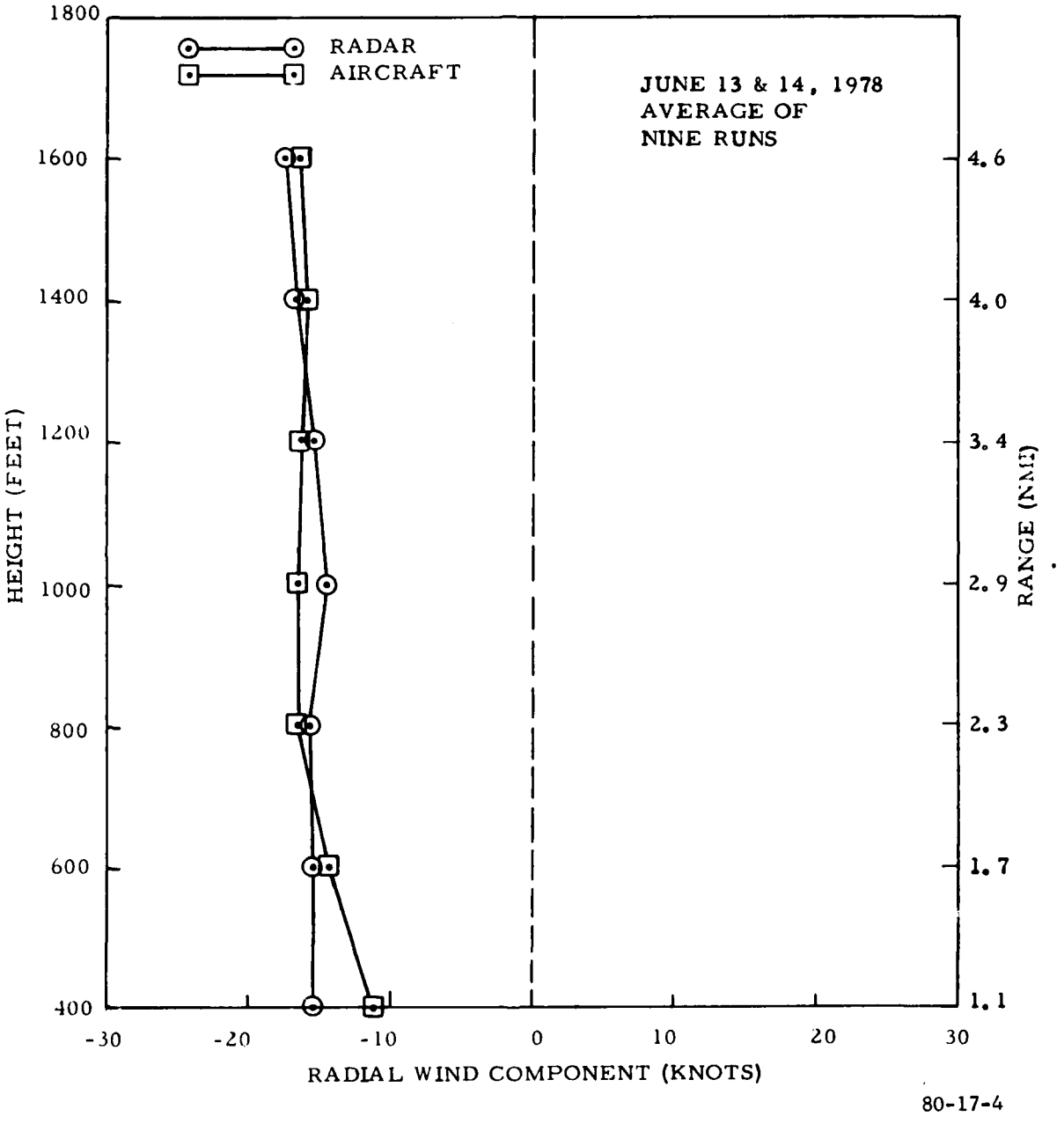

FIGURE 4. RADAR/AIRCRAFT COMPARISON--OUTBOUND, CLEAR AIR, NORTHWEST WINDS

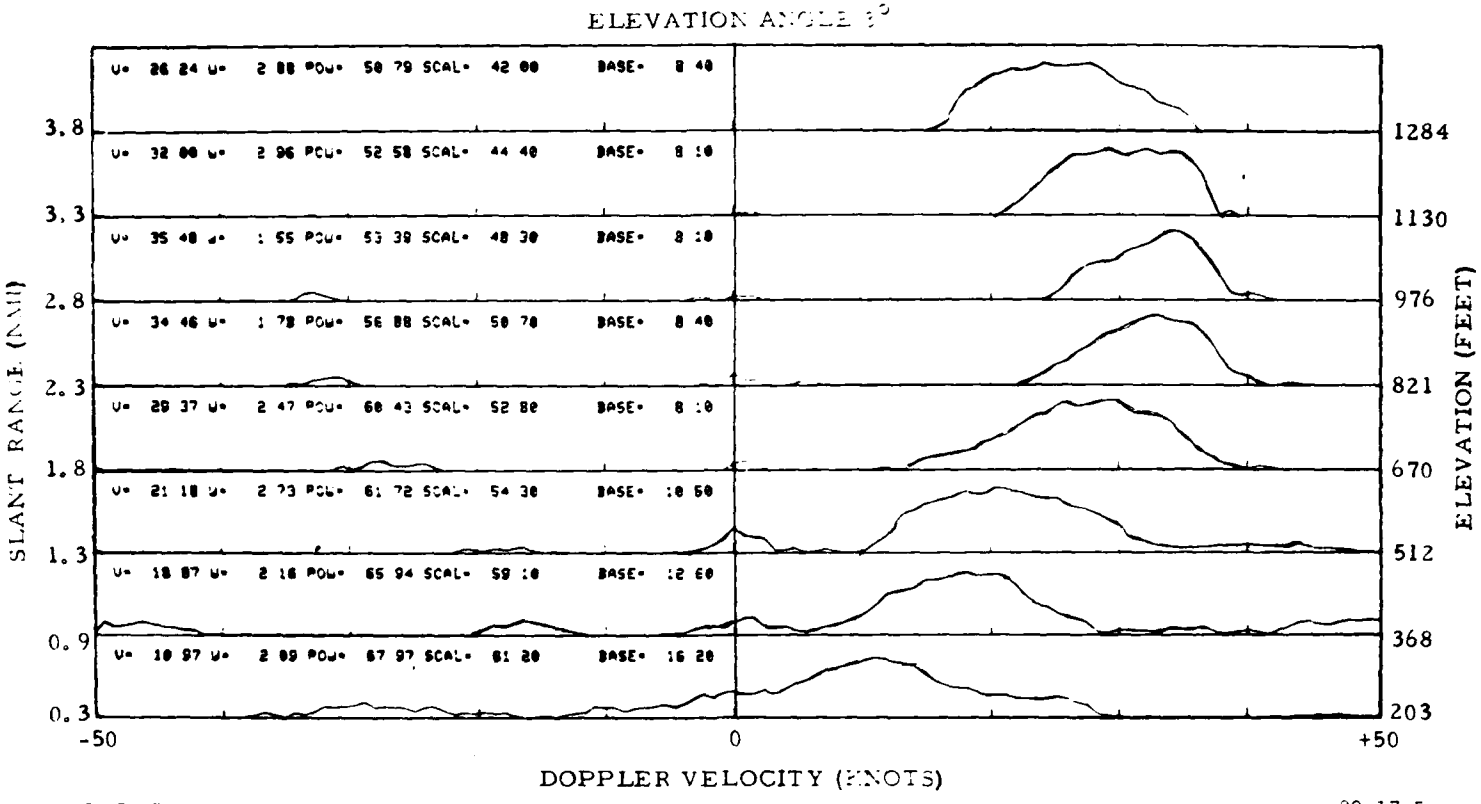

LEGEND:

V = SIGNAL MEAN RADIAL VELOCITY (KNOTS)
W = SIGNAL SPECTRUM WIDTH (KNOTS)
(STANDARD DEVIATION OF VELOCITY SPECTRUM)
POW = RELATIVE TOTAL SIGNAL POWER (dB)
SCAL = MAXIMUM DISPLAY RELATIVE POWER (dB)
BASE = DISPLAY BASE RELATIVE POWER THRESHOLD (dB)

FIGURE 5. PRECIPITATION SPECTRA

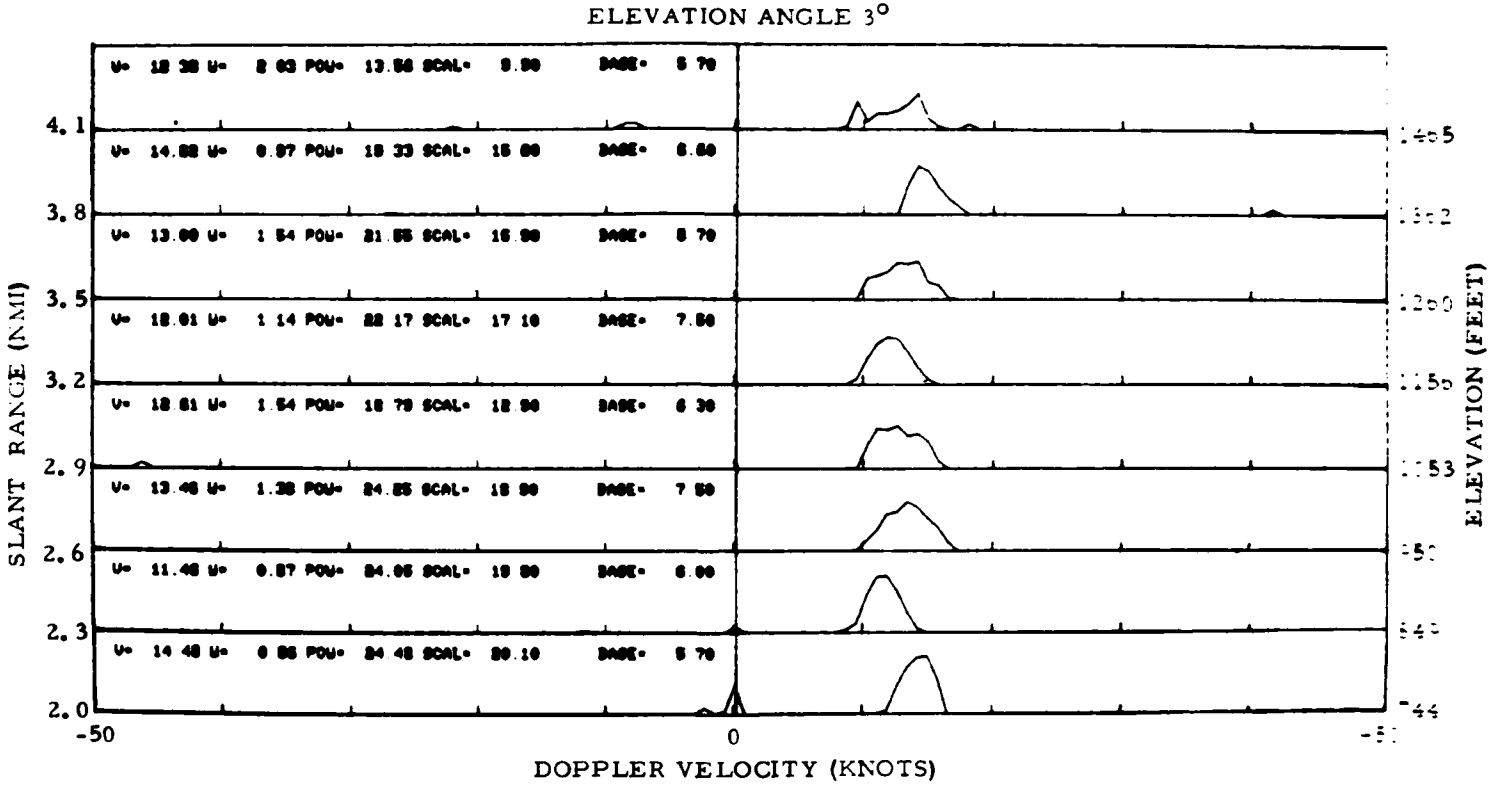

LEGEND:
V = SIGNAL MEAN RADIAL VELOCITY (KNOTS)
W = SIGNAL SPECTRUM WIDTH (KNOTS)
(STANDARD DEVIATION OF VELOCITY SPECTRUM)
POW = RELATIVE TOTAL SIGNAL POWER (dB)
SCAL = MAXIMUM DISPLAY RELATIVE POWER (dB)
BASE = DISPLAY BASE RELATIVE POWER THRESHOLD (dB)

FIGURE 6. CLEAR AIR SPECTRA

winds. The radar measured the wind components for discrete altitude levels just ahead of the aircraft as it descended. The radar and aircraft wind components for the glide slope azimuth were compared. (2) The aircraft flew actual approaches to runway 13-31 while radar data were taken on two azimuths spaced 30° apart, covering the runway approach area. Vector winds were computed for discrete altitude levels from wind components on the two azimuths. This two-azimuth pointing technique as discussed by Strauch (reference 2) is shown below:

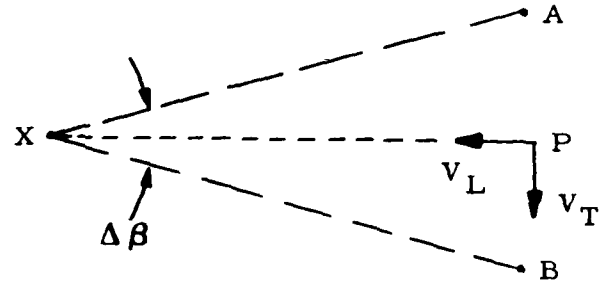

The two data azimuths are XA and XB. The angle between them is $\Delta\beta$. The wind is assumed to be locally constant; i.e., the same at P, A, and B. The wind vector is resolved into orthogonal components at P—the longitudual (V_L) and the transverse (V_T). By restricting measurements to small elevation angles, the fall velocities of precipitation particles may be neglected. This is equivalent to assuming a 0° elevation angle and results in the following equations for V_L and V_T:

$$V_L = \frac{V_A + V_B}{2 \cos\left(\frac{\Delta\beta}{2}\right)} \qquad V_T = \frac{V_A - V_B}{2 \sin\left(\frac{\Delta\beta}{2}\right)}$$

where V_A and V_B are the measured radial components at points A and B. Actually, V_L could be measured directly at P, although this was not done because of the additional processing time required. With faster computer facilities, a comparison of V_L measured at P and in terms of V_A and V_B would detect any horizontal variation of the wind and, thus, the nonvalidity of the two-point method. The angle between the measurements was 30° which provides a reliable measurement of V_T (under horizontally homogeneous wind conditions) while restricting the area of measurement horizontally. A superior technique is the Velocity-Azimuth Display (VAD), reference 3, which can provide accurate wind measurements over a larger area even if the horizontal wind varies linearly. Nonlinear horizontal wind changes can also be detected. This method involves measuring the radial velocity as a function of azimuth (continuously or discretely) and Fourier analyzing of the mean radial velocity at each height. However, this would require considerably larger computer facilities, although restricting measurements to precipitation would appreciably reduce this requirement.

The two-azimuth pointing technique provides wind speed from V_L and V_T. Wind directions are determined by appropriate trigonometry. The radar and aircraft headwind/tailwind and crosswind components for the runway azimuth were computed and compared.

It is important to emphasize that the two-azimuth pointing technique is applicable only to horizontally homogeneous winds and also, as pointed out in reference 4, should not be used where complex 3-dimensional wind fields are expected. Procedures for determining whether or not horizontal wind gradients are negligible will be formulated, tested, and evaluated during the 1980 test program.

Simulated Approaches. Radar data were obtained for eight levels from 1,600 to 300 feet above ground level (AGL) (close to mean sea level (MSL) for the Technical Center). The INS aircraft winds corresponding to the altitude levels at which radar data were measured were extracted from the aircraft data printouts. A FORTRAN computer program computed the aircraft headwind/tailwind components and produced statistical summaries comparing radar and aircraft

components. The totals for groups of approaches are shown in table 1. The totals for the groups of runs do not equal the number of approaches multiplied by eight. This is due to some radar wind signals being obscured by spurious targets or ground clutter (applies also to tables 3 and 4). Data are averages in knots for eight altitudes from 1,600 to 300 feet. Sigma is the standard deviation of radar minus aircraft component differences. (Radar components are negative for incoming winds.)

Table 1 shows that the radar components averaged 1 to 3 knots larger than the aircraft components, with standard deviations of about 3 knots. The agreement is better than that obtained previously in comparing Doppler-derived aircraft components with the ASR-8 Doppler components (reference 1).

A presentation of the data in table 1 grouped for each altitude level is shown in table 2. This shows the quasi-uniformity of agreement between radar and aircraft measurements over the various altitude levels.

Actual Approaches to 13-31. The ASR-8 installation is located 1.35 nautical miles (nmi) south-southwest of runway 13-31, nearer approach 31 than approach 13. The orientation of the runway, the radar location, and the data azimuths for the two approach areas are shown in figure 7.

Radar data were taken for eight altitude levels from 1,100 to 200 feet. The elevation angle for approach 13 surveillance was 1.6°, and for approach 31, it was 2°. These values were dictated by the radar offset location. Since data were taken on two azimuths, radar processing was started about 2 minutes before aircraft arrival and continued for 2 minutes after the approach was concluded. Total radar data collection time which included processing and display time and time to move the antenna was about 6 minutes. (This time can be reduced considerably with larger computer facilities.) Also, due to the radar offset (large compared to many field facilities), the radar was for the most part not measuring the wind components at the position of the aircraft. The best match was near 500 feet altitude on the glide slope. Quasi-horizontal space and time wind homogeneity was assumed based on existing meteorological conditions during the flight. However, wind gustiness did effect the data (tables 3 and 4).

A FORTRAN computer program computed the radar winds and also the radar and aircraft headwind/tailwind and crosswind components for the glidepath approach azimuths and produced statistical summaries. The totals for two groups of approaches are shown in table 3 (headwind/tailwind comparison) and table 4 (crosswind comparison). The first set of data was for approach 31, the second set was for approach 13. Data are averages in knots for eight altitudes from 1,100 to 200 feet. Sigma is the standard deviation of radar minus aircraft differences.

Table 3 shows that the radar components averaged slightly smaller than the aircraft components, with standard deviations of differences somewhat larger than for the comparisons of table 1. The larger sigmas were probably due to transitory wind changes caused by wind gustiness. This would affect the two sets of measurements differently due to space/time differences and differences in measuring procedures.

Table 4 shows that the average crosswind differences are small, but the standard deviations of differences are somewhat larger than with the headwind/tailwind comparisons of table 3. This is to be expected since the data azimuths are oriented more nearly parallel to the wind vector than orthogonal to it.

TABLE 1. COMPARISON OF RADAR AND AIRCRAFT WIND COMPONENTS FOR SIMULATED APPROACHES

RADAR*	A/C*	DIFF*	SIGMA*	APPCHS	TOTAL
-7.8	-5.6	-2.2	2.9	5	34
-19.5	-18.5	-1.0	2.9	5	35
-14.7	-11.8	-2.9	2.6	5	31

*Values are in knots.

TABLE 2. PRESENTATION OF THE DATA IN TABLE 1 GROUPED BY ALTITUDE

HEIGHT (ft)	RADAR*	A/C*	DIFF*	SIGMA*	DIST**	TOTAL
1,600	-14.2	-12.2	-2.0	2.8	4.6	11
1,400	-14.2	-13.1	-1.1	3.0	4.0	14
1,250	-14.9	-12.2	-2.8	3.5	3.5	14
1,050	-14.5	-12.2	-2.4	3.6	2.9	13
900	-14.0	-12.1	-1.9	2.7	2.3	15
700	-14.6	-12.3	-2.3	2.2	1.8	10
500	-13.3	-11.7	-1.6	3.0	1.2	12
300	-12.2	-10.4	-1.8	2.3	0.6	11
ALL	-14.0	-12.1	-2.0	2.9	---	100

*Values are in knots.
**Nautical miles from radar

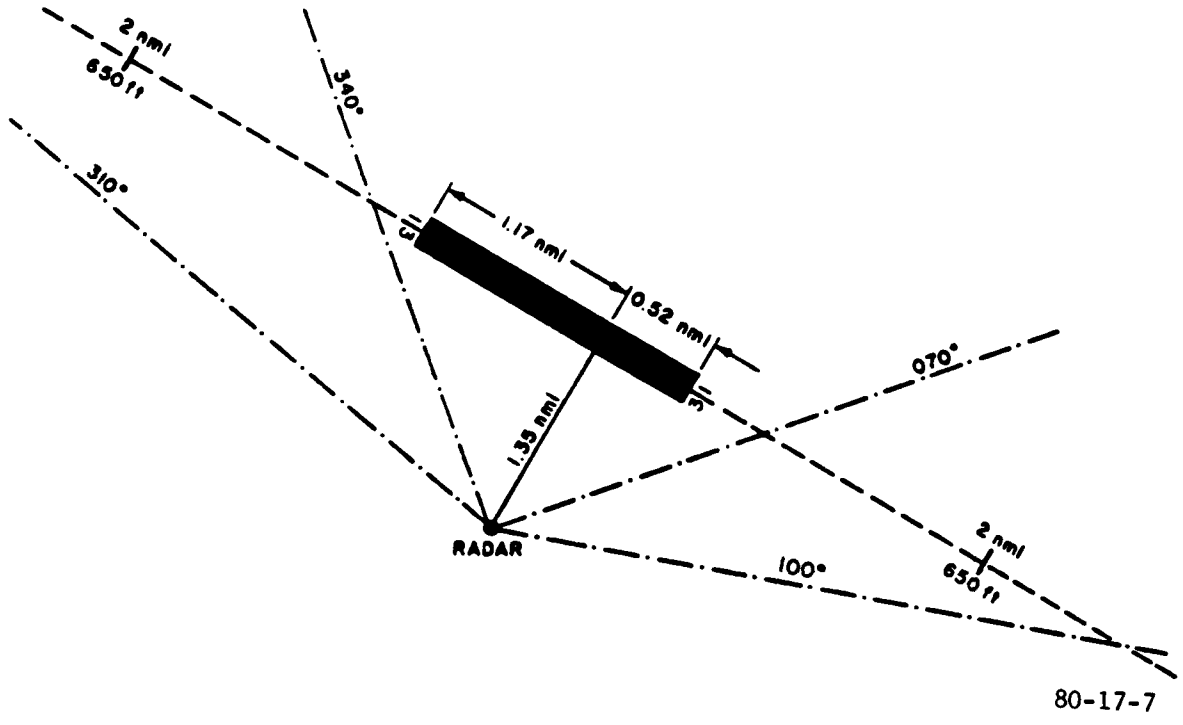

FIGURE 7. RUNWAY 13-31, RADAR LOCATION AND DATA AZIMUTHS FOR WIND DETERMINATION

TABLE 3. COMPARISON OF RADAR AND AIRCRAFT HEADWIND/TAILWIND COMPONENTS FOR ACTUAL APPROACHES

RADAR*	A/C*	DIFF*	SIGMA*	APPCHS	TOTAL
18.4	18.8	-0.4	4.7	6	38
21.9	22.9	-1.0	3.2	5	33

*Values in knots, headwind positive

TABLE 4. COMPARISON OF RADAR AND AIRCRAFT CROSSWIND COMPONENTS FOR ACTUAL APPROACHES

RADAR*	A/C*	DIFF*	SIGMA*	APPCHS	TOTAL
-13.6	-13.2	-0.4	7.0	6	38
22.4	21.5	0.9	5.5	5	33

*Values in knots, right crosswind positive

RADAR/TOWER WIND COMPARISON. Radar winds determined by using the two-azimuth pointing technique were compared with winds from a tower-mounted sensor. The tower is a massive open-type triangular structure located 2 nmi due north of the radar. The tower is 163 feet high, and the wind sensor is mounted on a mast at a height of 178 feet. The sensor position on the tower and the tower orientation was such that the most accurate wind measurements would be expected with wind directions from 290° clockwise to 110°. The least accurate sector would be from 240° counterclockwise to 160°, with the remaining zones intermediate. No tests have been made comparing sensor readings with those from sensors mounted on extended booms so the tower effect can only be estimated.

The radar data azimuths were usually 345° and 15°. This resulted in the radar winds being calculated over a lateral distance of 1.1 nmi centered on the tower. Data were taken in the clear air, and in order to minimize returns from ground targets (primarily auto traffic), it was necessary to elevate the beam to a point approximately 200 feet above the tower.

The radar-measured wind components on each azimuth were approximately 1-second averages. Total cycling time for each set of measurements was 1 minute. This included processing and display time and time to move the antenna. The components were determined manually from the type of data shown in figure 6. Manual determination was required since it was necessary to use a nonstandard pulse repetition frequency (PRF), not compatible with the automatic program for computing mean velocity. Tower winds were averaged over a 1-minute period approximately every 8 seconds with output to the nearest 10° and 1 knot. The values closest to the radar 1-minute processing periods were extracted for comparison. Data collection periods were about 1 hour with radar/tower data pairs obtained on the average every 3 to 5 minutes. The actual intervals between successive comparisons depended upon the frequency of occurrence of false targets (birds, ground traffic, etc.) which obscured the wind signals.

The data were processed by a FORTRAN computer program that determined the radar winds and produced the statistical comparisons. Table 5 shows the average winds and the average wind direction/speed differences for discrete groups of observations. Table 5 shows that the average direction differences and speed differences expand with increasing wind speeds, and the standard deviations tend to become larger with increasing wind speed. This probably reflects some tower effect with the stronger winds, particularly since the best agreement is with the lightest wind sample even though directions are in the least reliable sector. Conditions were quite gusty for the last two groups. Gusty conditions would also contribute to the larger differences for those samples because of the different sampling times and altitude difference.

The radar/tower wind comparison demonstrates the accuracy with which horizontal wind can be determined by the radar.

THUNDERSTORM DATA. During the evening of August 10, 1979, observations were taken in precipitation associated with a thunderstorm as it moved from west to east over the radar site. A check of the National Weather Service (NWS) observations from the weather station at the FAA Technical Center showed that no gust front was associated with this thunderstorm. However, some strong radial shears (variations of radial wind components along the pointing direction of the radar beam) were observed. Tables 6 to 10 show data for a sequence of observations. The levels are in feet AGL with distances from the radar in

TABLE 5. RADAR/TOWER AVERAGE WINDS AND DIRECTION/SPEED DIFFERENCES

RADAR	TOWER	DIR DIFF	DIR SIGMA	SPD DIFF	SPEED SIGMA	TOTAL
228/12	230/10	-3.0	11.5	1.2	1.8	14
315/14	321/12	-4.6	14.7	2.0	2.7	10
315/19	327/15	-10.3	12.6	4.2	5.3	22
309/25	326/20	-14.8	12.9	5.1	6.9	22

NOTE: Data are averages for discrete groups.
Directions are in degrees.
Speeds are in knots.
Sigmas are the standard deviations of differences.

TABLE 6. THUNDERSTORM OBSERVATION AT 1941 EDT, AZIMUTH = 299°, ELEVATION = 2°

LEVEL	COMP	RADIAL SHEAR	DIST
924	-23.0	---	3.9
866	-22.0	1.7	3.6
787	-21.0	1.3	3.2
718	-22.0	-1.4	2.9
650	-12.0	14.7	2.6
581	-13.0	-1.4	2.3
512	-11.0	2.9	1.9
444	-9.0	2.9	1.6

NOTE: Levels are in feet AGL.
Wind components are in knots (negative toward the radar).
Radial shears are in knots per 100 feet.
Distances are in nautical miles from the radar.

TABLE 7. THUNDERSTORM OBSERVATION AT 1954 EDT, AZIMUTH = 300°, ELEVATION = 3°

LEVEL	COMP	RADIAL SHEAR	DIST
1,285	-38.0	-2.6	3.9
1,130	-40.0	-1.3	3.4
976	-42.0	-1.3	2.9
821	-28.0	9.0	2.4
667	-33.0	-3.2	1.9
512	-23.0	6.5	1.5
358	-23.0	0.	1.0
203	-18.0	3.2	0.5

NOTE: Levels are in feet AGL.
Wind components are in knots (negative toward the radar).
Radial shears are in knots per 100 feet.
Distances are in nautical miles from the radar.

TABLE 8. THUNDERSTORM OBSERVATION AT 1956 EDT, AZIMUTH = 300°, ELEVATION = 3°

LEVEL	COMP	RADIAL SHEAR	DIST
2,521	-30.0	----	7.8
2,367	-31.0	-0.6	7.3
2,212	-25.0	3.9	6.8
2,058	-17.0	5.2	6.3
1,903	-33.0	-10.3	5.8
1,748	-49.0	-10.3	5.3
1,594	-50.0	-0.6	4.9
1,439	-34.0	10.3	4.4

NOTE: Levels are in feet AGL.
Wind components are in knots (negative toward the radar).
Radial shears are in knots per 100 feet.
Distances are in nautical miles from the radar.

TABLE 9. THUNDERSTORM OBSERVATION AT 2003 EDT, AZIMUTH = 80°, ELEVATION = 3°

LEVEL	COMP	RADIAL SHEAR	DIST
1,285	36.0	----	3.9
1,130	30.0	-3.9	3.4
976	36.0	3.9	2.9
821	36.0	0	2.4
667	39.0	1.9	1.9
512	30.0	-5.8	1.5
358	21.0	-5.8	1.0
203	21.0	0	0.5

NOTE: Levels are in feet AGL.
Wind components are in knots (negative toward the radar).
Radial shears are in knots per 100 feet.
Distances are in nautical miles from the radar.

TABLE 10. THUNDERSTORM OBSERVATION AT 2010 EDT, AZIMUTH = 80°, ELEVATION = 3°

LEVEL	COMP	RADIAL SHEAR	DIST
1,285	37.0	----	3.9
1,130	24.0	-8.4	3.4
976	22.0	-1.3	2.9
821	21.0	-0.6	2.4
667	15.0	-3.9	1.9
512	23.0	5.2	1.5
358	22.0	-0.6	1.0
203	18.0	-2.6	0.5

NOTE: Levels are in feet AGL.
Wind components are in knots (negative toward the radar).
Radial shears are in knots per 100 feet.
Distances are in nautical miles from the radar.

nautical miles. Wind components are in knots; incoming winds have negative values. Radial shear is in knots per 100 feet of altitude along the radar beam and is determined by subtracting lower level values from upper level values for successive gates and dividing by the absolute altitude difference in hundred's of feet.

Table 6 shows data for the first observation as the storm approached from the west. A sharp shear was found at about 700 feet separating quasi-uniform incoming wind components above and below that level. Tables 7 and 8 show a continuous altitude sequence from 200 to 2,500 feet. Winds increased relative to those of table 6 and built to a peak of 50 knots near 1,600 feet. There is considerable wind variation with altitude producing variable shears, some quite large. The shear variation is an indication of the intense convective activity within the storm at scale size which can be resolved by the radar. The peak of the storm was reached about this time. Key elements of the official NWS observation for 1955 Eastern Daylight Time (EDT) taken at a point about 1.1 nmi northeast of the radar were: estimated 1,200-foot overcast, 1/2-mile visibility in a heavy thunderstorm (TRW+) with haze, wind 280° at 13 knots. Tables 9 and 10 show radar observation on an easterly bearing as the storm was passing by. The shear below 700 feet in table 7 essentially shows up with opposite sign in table 9. In table 10 winds are diminishing, but some strong shears persist.

This group of observations shows that radial shear in thunderstorms can be detected by the radar system. Additional thunderstorm observational sequences are planned for the spring and summer of 1980. It is expected that gust fronts will occur, and they will be investigated in detail.

SQUALLY WEATHER WIND SHEAR. A period of squally weather in advance of a cold front occurred at the Technical Center from about 1000 to 1600 on November 26, 1979. Surface winds were generally 170° at 22 knots with frequent sustained gusts of 30 knots. Visibilities were generally near 1 mile in light rain and fog with ceilings mostly overcast, about 500 feet. Shortly after 1600 the wind shifted to the south/southwest and dropped to steady values below 20 knots (no gusts). The cold front passed through rapidly just after 1800, with a brief period of strong winds and a peak gust of 44 knots from the west. During part of the squally weather period, a series of radar wind measurements were made at eight levels from 250 to 1,700 feet on azimuths oriented approximately into or with the wind. The peak wind components at 1,700 feet varied from 55 to 70 knots. Those at 250 feet were generally 15 to 25 knots. Some moderate-to-strong radial shears were consistently observed for discrete 200-foot layers, mostly below 1,050 feet. Aircraft descending on an approach into the wind would have experienced some abrupt airspeed loss under these conditions. This is shown by the plots of figures 8 and 9. Figure 8 shows the larger of the two shears in knots per 100 feet for the 1,050- to 850-foot layer or the 850- to 650-foot layer. Figure 9 shows the larger of the two shears from 650 to 450 feet or 450 to 250 feet. Considered in combination with the low ceilings and visibilities and gusty surface winds, these shears cannot be taken lightly. Figures 8 and 9 are considered to be representative for the 1000 to 1600 period. Continuous radar wind shear observations would be of value under such conditions. More work is needed to determine possible operational applications.

SYSTEM CAPABILITIES AND LIMITATIONS. Doppler radar techniques for wind measurement are reviewed in reference 4, which discusses the capabilities and limitations applicable to systems such as the Technical Center ASR-8 Wind Shear Detection System. Some

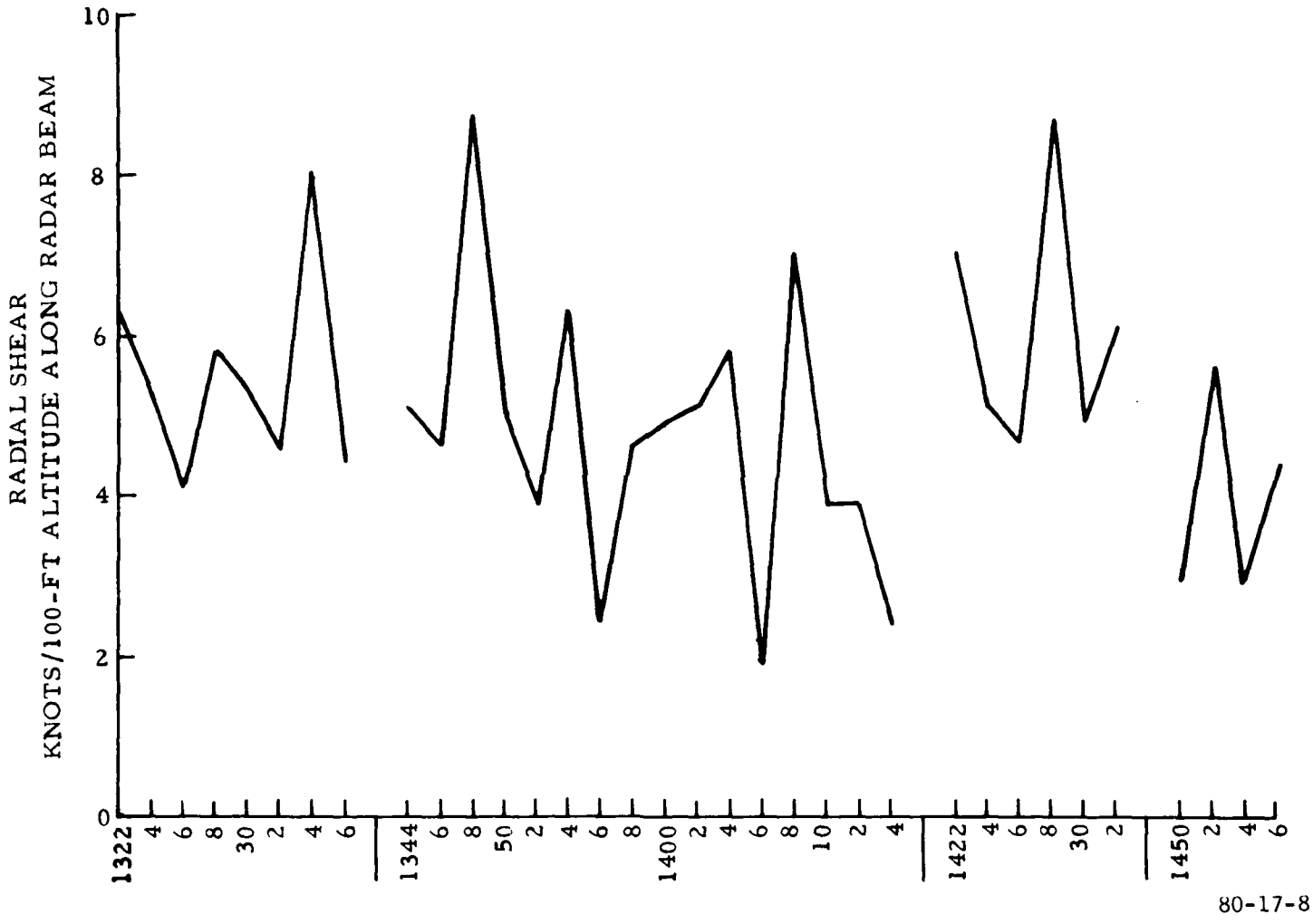

FIGURE 8. TIME HISTORY OF MAXIMUM RADIAL SHEAR OBSERVED IN THE 650- TO 1,050-FOOT LAYER BY RADAR

FIGURE 9. TIME HISTORY OF MAXIMUM RADIAL SHEAR OBSERVED IN THE 250- TO 650-FOOT LAYER BY RADAR

additional findings determined during the course of evaluation at the Technical Center are highlighted in the ensuing paragraphs as well as in excerpts from the literature.

Meteorological and ATC Use of Doppler Wind Data. Wind is one of the most important meteorological parameters used by the meteorologist in making weather forecasts. The only upper-air wind data available routinely are from radiosonde runs made twice each day (00Z and 12Z) for a limited network of weather stations. Aircraft are a source of nonroutine wind data. An operational Doppler wind shear alert system could provide additional data when rapid update of wind shear information was not required. An example of this is shown in table II. The winds were determined by measuring radar wind components on azimuths of 30° and 60° during an unusual snowstorm moving from the northwest over south central New Jersey.

The precipitation was caused by the overrunning of cold northeast to east winds at lower levels by warmer, moister southeast to south winds at higher levels. The consistency of wind direction change indicates that the assumption of horizontal wind homogeneity (required by two-azimuth pointing technique) was valid for these observations. A sequence of such observations could provide trend information very useful in forecasting the intensity and duration of the precipitation.

Table 12 shows another sequence taken in pre-cold frontal rain. Particularly interesting is the peaking of the windspeed near 3,000 feet. The erratic directional variation at the lower levels indicates that the winds were not horizontally constant. However, wind gustiness may have been a contributing factor. A second sequence (not shown) which extended observations to 10,000 feet showed remarkably constant winds above 5,000 feet (245° to 250° at 58 knots). This type of wind information would be useful for planning approach to and departure from terminal areas.

Hardware/Software Limitations. Except for the range gate generator and buffer memory provided by WPL, the rest of the equipment was made available from a previous Technical Center project. Thus, the system was not designed from an optimum standpoint. Instead, the objective was to demonstrate the feasibility of measuring winds with an FAA radar as economically as possible and to defer development of new data processing equipment and software until the technique has been proven feasible and desirable from an operational viewpoint. Much work remains to be done, though some improvements have already been made or have been planned. A new display has been installed, improved data display and reduction programs have been developed, and other software improvements are being formulated. Some recommendations for further improvement, found in reference 4, include the addition of an array processor for increased data rate, a color display, and a multimoment display.

Antenna Limitations. One of the primary and most costly items required to modify the ASR-8 for wind shear measurements is the parabolic antenna and its associated pedestal assembly which is shown in figure 2. For example, the total cost of the parabolic antenna and pedestal assembly was approximately $270,000, excluding the cost of waveguide sections required for installation and a waveguide hot air dryer unit. The dryer unit was found to be necessary to preclude arcing in the antenna feed assembly with full transmitter power applied under certain atmospheric conditions.

Since the pedestal assembly is the most expensive component by far ($247,000), future test efforts will be directed toward optimization of antenna

TABLE 11. RADAR WIND OBSERVATIONS IN SNOW, AZIMUTH = 45°, ELEVATION = 9°

LEVEL	WIND	DIST
4,719	181/19	4.9
4,104	167/17	4.2
3,488	146/16	3.6
2,872	128/14	2.9
2,256	100/12	2.3
1,640	082/10	1.6
1,024	079/14	1.0
408	034/10	0.3
Surface	030/7	(NWS observation)

NOTE: Levels in feet MSL
Wind in degrees/knots
Distances in nautical miles from the radar

TABLE 12. RADAR WIND OBSERVATIONS IN RAIN, AZIMUTH = 45°, ELEVATION = 9°

LEVEL	WIND	DIST
4,719	239/56	4.9
4,104	237/56	4.2
3,488	239/67	3.6
2,872	228/71	2.9
2,256	218/67	2.3
1,640	229/53	1.6
1,024	205/40	1.0
408	242/30	0.3
Surface	210/22	(NWS observation)

NOTE: Levels in feet MSL
Wind in degrees/knots
Distances in nautical miles from the radar

pointing directions with the aim of eliminating the need for similar pedestals in field use.

Axial power density measurements were performed in the antenna near-field by a member of the Spectrum Management Staff, ARD-60, and are discussed in reference 5. Pertinent information is noted below.

1. ASR-8 transmitting conditions:

a. Frequency - 2790 megahertz (MHz)

b. Peak pulse power - 1 megawatt (MW)

c. Waveguide loss - (100 feet) approximately 1 decibel (dB)

d. Pulse width - 0.6 microsecond (μs)

e. PRF (uniform) - 1030

f. Duty cycle - 1030 x 0.6 μs = 0.000618

g. Power average = 10^6 x 0.7943 x 0.000618 = 491 watts

2. Wind shear/turbulence antenna characteristics:

a. Purchased from and tested by Microwave Specialty Corporation (MSC), San Diego, California 92123. Uses a specially designed feed with a Prodelin standard parabolic fiberglass reflector, Prodelin Part No. PA179-93, 15-foot diameter (72-inch focal length).

b. Polarization - vertical

c. Beam widths (measured by MSC at 2.8 gigahertz (GHz))

- Vertical (E) 1.6°
- Horizontal (H) 1.75°

d. Antenna gain 38 dB (6,310) (measured by MSC at 2.8 GHz)

e. Side-lobes at least 26.5 dB down

The power density instrumentation consisted of a Narda model 8323 Broadband Isotropic Probe connected to a Narda model 8306 Radiation Monitor with the supplied 6-foot extension cable. The 15-foot antenna was fixed mounted at a height of approximately 40 feet pointing up 3° in elevation. At each measurement distance the bucket of the HI-RANGER was positioned below (and sometimes to the side of) the beam. The Narda model 8323 probe, secured to a stick, was then positioned within the beam for maximum indication on the radiation monitor. The distances were manually paced.

Measured data:

Distance from antenna (feet)	Power Density (mW/cm^2)
310	5
220	7.5
160	9.0
150	8.5
135	7.5
75	8.3
60	13
50	9
40	11
30	9
25	11
20	10

A discussion of these test results in reference 5 reveals evidence of possible instrumentation errors which could reduce the measured power density to half in each case. For information, the FAA standard with regard to electromagnetic radiation states that levels above 10

milliwatts per centimeter squared (mW/cm^2) are considered to exceed the safety threshold.

Performance Limitations. Most of the basic performance limitations are discussed in considerable detail in reference 6. In general, they can be divided into two separate categories; i.e., radar design constraints and signal/false alarm detection problems.

Some of these problems may be amenable to solution, while others may not. Therefore, as with any radar development, operational use may necessitate some performance trade-offs.

The primary limitation of the two-azimuth radar pointing technique is the requirement for horizontal wind homogeneity. Most serious wind shear situations are associated with thunderstorm downbursts and gust-fronts. These are conditions which produce strong vertical and horizontal shears that cannot be measured with the two-azimuth pointing technique.

Antenna Beam Width and Radar Offset. The mean Doppler velocity depends on the radial velocity distribution of the scatterers in the radar resolution cell. Thus, the radar-measured velocity is the antenna beam-filtered version of the actual wind component along the axis of the radar beam. Velocity gradients existing over distances much smaller than the radar antenna beam width will cause a broadening of the Doppler spectrum but will not be revealed by the radar-measured mean velocity.

Velocity gradients existing over distances comparable with the beam width will be integrated over the antenna beam so that peak values will not be detected. Furthermore, if the radar is offset from the runway so that the axis of the radar beam is parallel to but displaced from the flightpath, the measured wind component will be representative of the actual wind component along the flightpath only if the wind field is horizontally homogeneous (i.e., if there are no horizontal gradients such as those associated with thunderstorms).

Reference 7 describes a computer simulation for testing the effects of both finite radar resolution volume and radar displacement relative to the runway on the radar-measured component of the wind along the flightpath. The simulation program contains six wind shear models, and the results obtained with these models are included in that report.

The following is quoted from the Conclusions Section of reference 7:

"The simulation results show that for an antenna beamwidth of 1.5 degrees, low-level gradients in realistic wind profiles will be properly measured by the radar. If the wind field does not contain significant horizontal gradients, the elevation angle is not critical. The results suggest that one way to test whether horizontal gradients are important is to measure the profile at various elevation angles. At an elevation angle equal to the glide slope (nominally 3 degrees), strong gradients at a 500-m altitude will be heavily filtered by the radar pulse volume, because of the vertical extent of the antenna beamwidth. Therefore, this strong filtering will remain until the elevation angle is very high, and, since the minimum range of a pulse radar is at least several microseconds, it will not be possible to resolve strong gradients at altitudes above several hundred meters. The antenna beamwidth filters the wind profile, but does not significantly filter realistic wind profiles at low levels.

"The effect of radar offset from the runway presents a serious problem for wind fields with significant horizontal gradients commonly found in thunderstorms. It is evident from these simulations that the profile along a path parallel to the glidepath

is not acceptable for offsets of several kilometers. If there is a precipitation echo, the entire region may be scanned (rapidly) and a single Doppler radar may be able to identify hazardous areas without actually measuring the wind vector." (See references 4 and 6 for additional analysis.)

Ambiguities. Much attention has been paid to the range-velocity ambiguity problem both in terms of definition and schemes for alleviation. Conventional radar designs exist which can handle ambiguities when targets are limited in size, scope, and number but do not work well with metorological targets. Figure 10 shows an example of range-ambiguous thunderstorm cells seen by the ATC channel of the Technical Center wind shear radar. These range-overlaid echoes can be recognized by their radially elongated shape. Target range is ambiguous when true range exceeds $cT_s/2$ (where c is propagation speed, 3×10^8 meters per second, and T_s is the radar pulse repetition time).

These range-ambiguous signals can mix with or completely obscure the desired near-range signals producing erroneous mean velocity estimates.

Figure 11 shows the same ATC display as in figure 10 but with the high-beam antenna in use. (The ASR-8 employs a dual-beam antenna.) The range-ambiguous returns are nearly gone. This illustrates the effects of higher elevation angles on this type of unwanted signal. This is a potential solution for use when winds are horizontally homogeneous.

Errors can also result because the radar cannot distinguish between real Doppler shifts and those spaced in frequency by multiples of the PRF. Figure 12 is a sample of ASR-8 spectral data recorded during a snowstorm that shows the mean velocity progressing from -21 knots to a point of "fold-over" then changing sign to a value of +32 knots. Once again, such data would produce velocity errors.

Antenna side-lobes can also cause "spatial" ambiguities. For example the antenna used in the Center's system produces two-way, range-measured side-lobe levels 50 to 60 dB below the main-lobe. Since meteorological signals can vary over ranges of as much as 80 dB, it can be seen that strong signals from precipitation located off to the side of the antenna main-lobe pointing direction can obscure or interfere with the desired clear-air signal.

Side-lobes also increase the ground clutter returns, though in general this form of clutter has not been a limiting factor at the Center. Methods to eliminate ground clutter which appear in the data centered around zero velocity are available for future use (figures 5, 6, and 13 through 15).

Anomalous Signal Returns. Standard ATC radars experience problems, often very severe ones, with interference from unwanted signals. Though most can be controlled through the use of various "fixes" and techniques, the most troublesome ones, caused by moving cars, birds and insects, are magnified with the wind shear radar because of its increased sensitivity. Also, most of these targets are at relatively low elevations, as seen in data collected with the antenna at 3°, and thus may be troublesome for wind measurements along the glidepath. However, since the targets are moving, they rarely remain in the same location from one sampling period to the next, suggesting the use of statistical sampling methods to reduce false alarms. The present system is limited to relatively slow data rates which would preclude the use of longer dwell times, but this can be improved with hardware and software designs.

Refractive Index Considerations. The radar's ability to detect winds in clear air arises from scattering due to refractive index variations in the atmosphere. These variations, denoted as the structure constant of

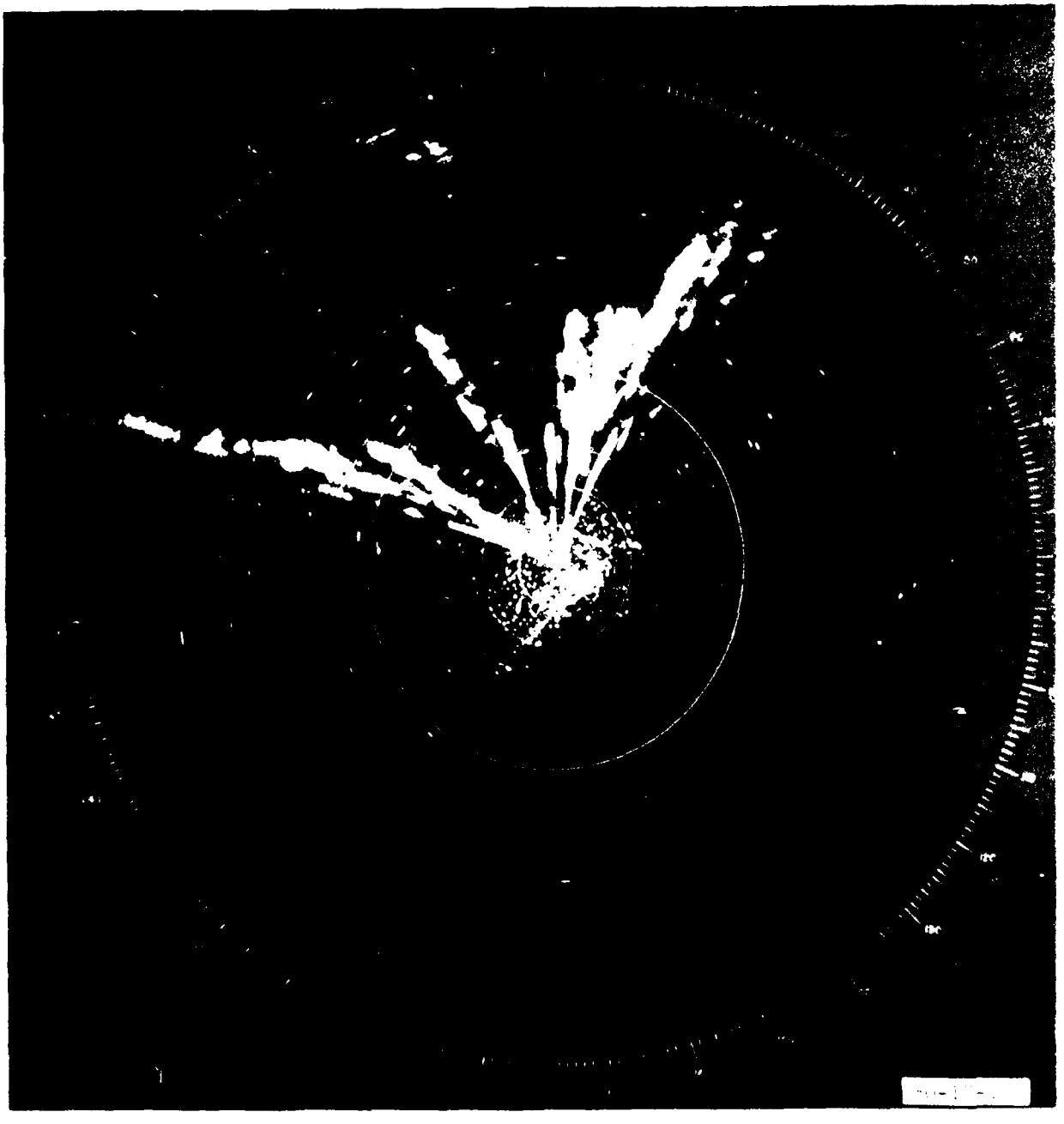

FIGURE 10. RANGE-AMBIGUOUS RETURNS WITH LOW-BEAM ANTENNA

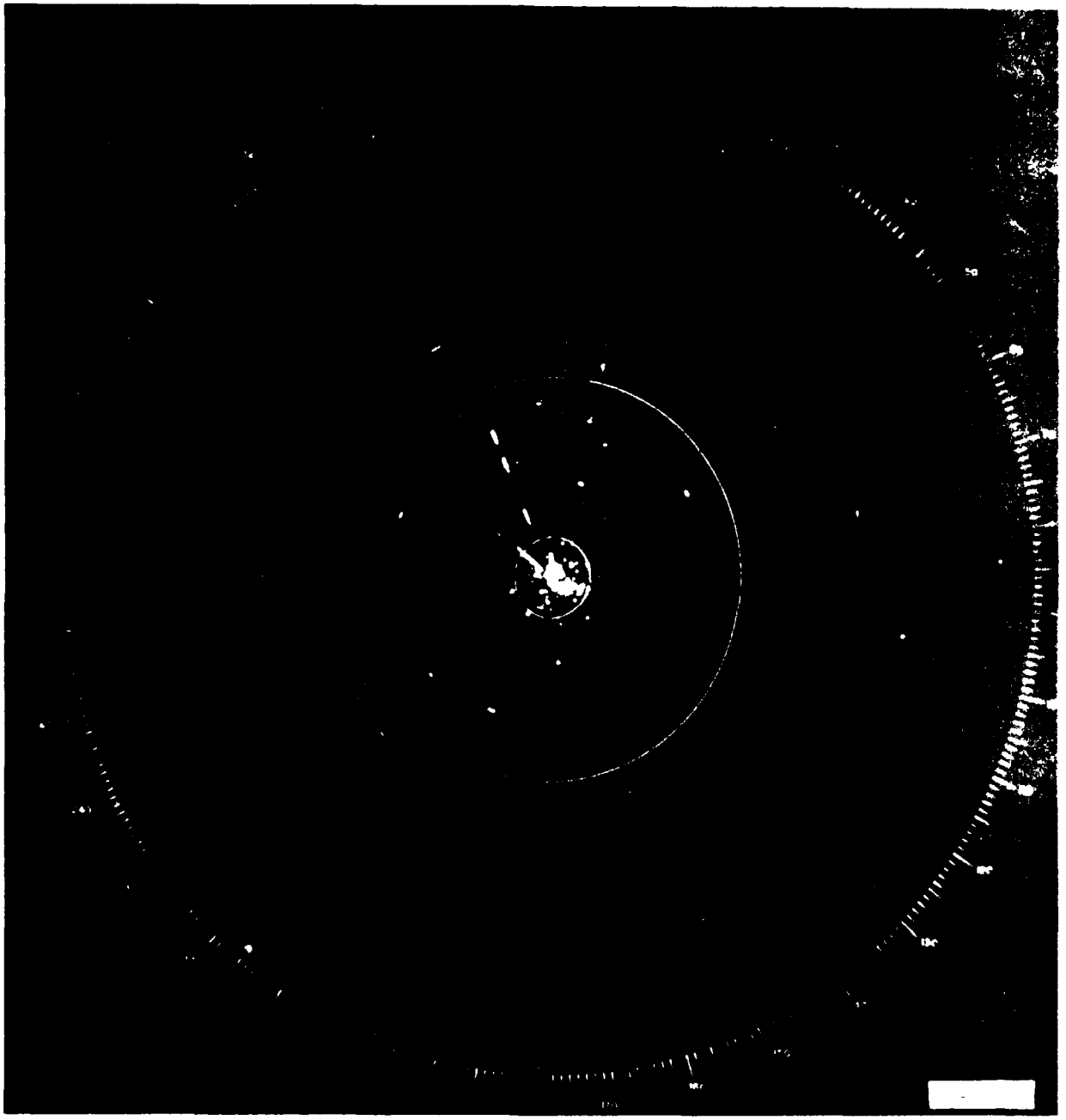

FIGURE 11. RANGE-AMBIGUOUS RETURNS WITH HIGH-BEAM ANTENNA

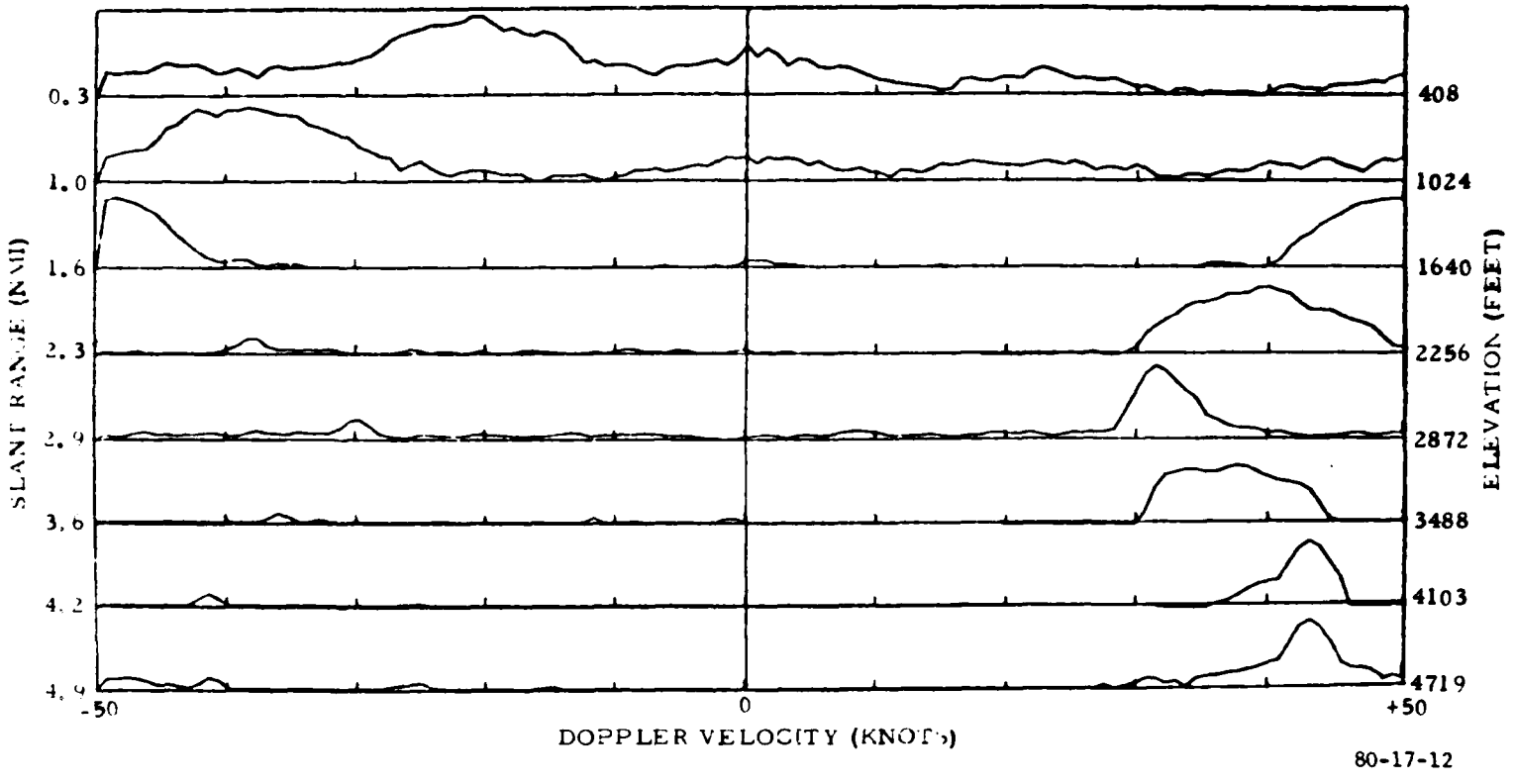

FIGURE 12. SPECTRAL DATA FROM A SNOWSTORM

radio-refractive index (C_n^2) are of a scale size ($\lambda/2$), to which the 10-centimeter ASR-8 is sensitive.

The level of C_n^2 varied over ranges as wide as 60 dB when measured by another microwave radar (reference 8) as a function of meteorological conditions, time of day, and time of year; lowest levels occuring in the winter with very dry clear air. Data taken at the Center showed a corresponding variation in clear-air spectral levels under similar conditions. Figures 13 through 15 illustrate the effects of antenna elevation angle on the detection of terminal area winds with marginal returns, indicating that higher elevation angles may be a solution to this problem, but may not be suitable for glidepath measurements.

SUMMARY OF SECOND PHASE RESULTS

1. In simulated approaches toward the radar site, radar-measured headwind/tailwind components averaged about 2 knots larger than those derived from aircraft winds.

2. In actual approaches to Center runway 13-31, radar-derived headwind/tailwind components averaged about 1 knot less than those derived from aircraft winds in horizontally homogeneous wind conditions. In the crosswinds comparison, radar values averaged about 1 knot more than the aircraft values. For these tests, the radar winds were derived from wind components measured on two azimuths separated by 30°.

3. In a comparison of radar winds measured 200 feet above a tower, with winds from a sensor mounted just above the tower top, the radar wind speeds averaged 1 to 5 knots greater than tower speeds. The speed differences increased with increasing mean wind speed. The radar wind directions averaged 3° to 15° less than tower directions, increasing with increased mean wind speed.

4. Radar observations in a thunderstorm and during a sustained squally period showed that potentially dangerous shears could be detected on a continuing basis. However, further investigation is needed to determine operational applications.

5. The application of radar-derived upper winds for weather forecasting as well as air traffic control was shown by observations taken in storm precipitation.

6. System limitations with regard to hardware/software, antenna problems and various performance factors were discussed, and solutions and/or trade-offs were considered.

CONCLUSIONS

Based on the results described, it is concluded that:

1. The Wave Propagation Laboratory (WPL) wind shear system operated satisfactorily with the Federal Aviation Administration (FAA) Technical Center Airport Surveillance Radar (ASR)-8, and the processing and spectral display of radar returns were shown to be feasible in both precipitation and the optically clear atmosphere.

2. Flight tests indicated the system is capable of measuring radial wind components along the simulated flightpath (radial to the radar) flown by the aircraft. Thus a radar located near a runway could measure headwinds or tailwinds along the path of landing or departing aircraft.

3. With the radar offset from the runway and with the horizontally homogeneous wind regimes encountered at the Center to date, the two-azimuth pointing method was capable of determining wind

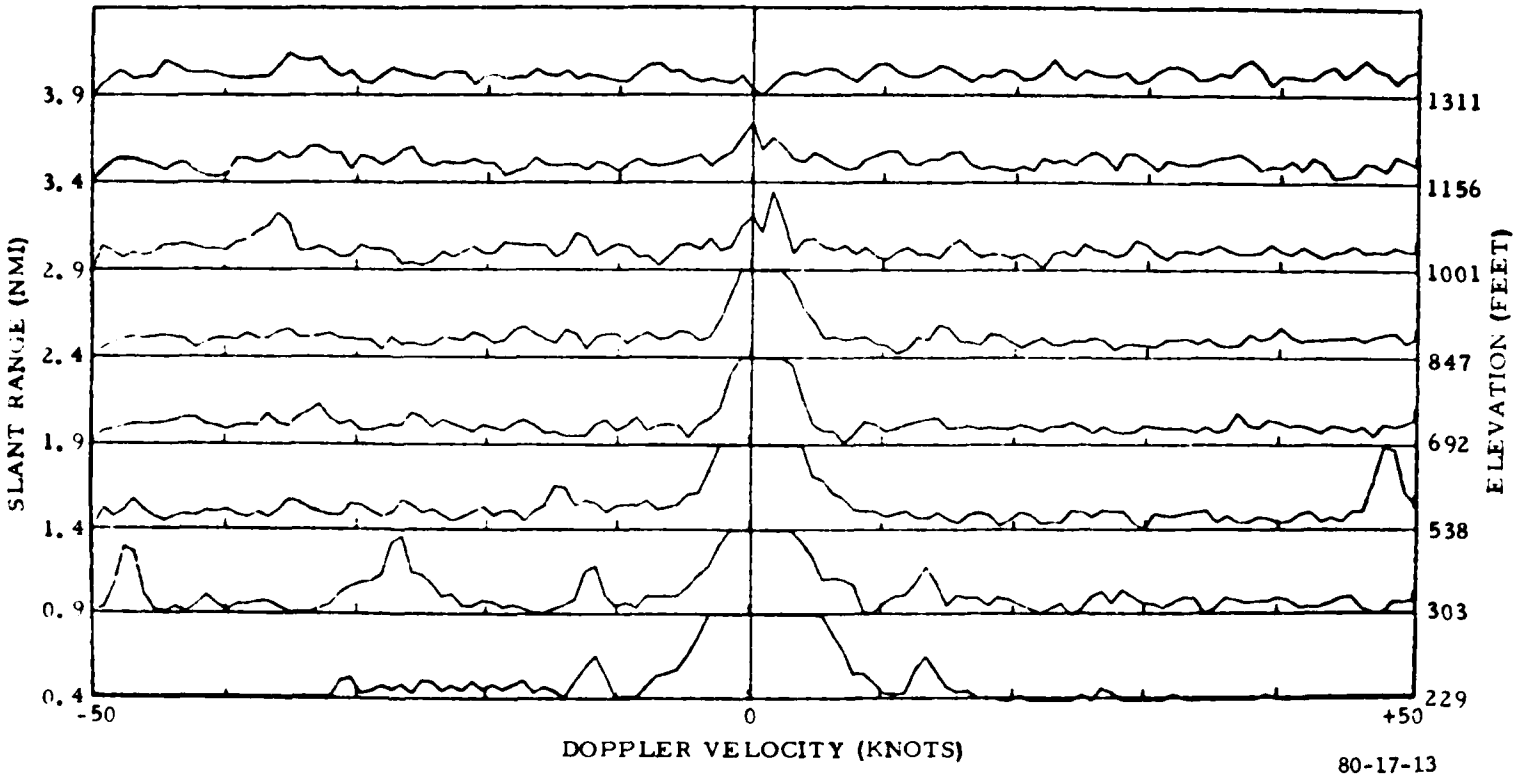

FIGURE 13. CLEAR AIR SPECTRA AT 3-DEGREE ELEVATION ANGLE

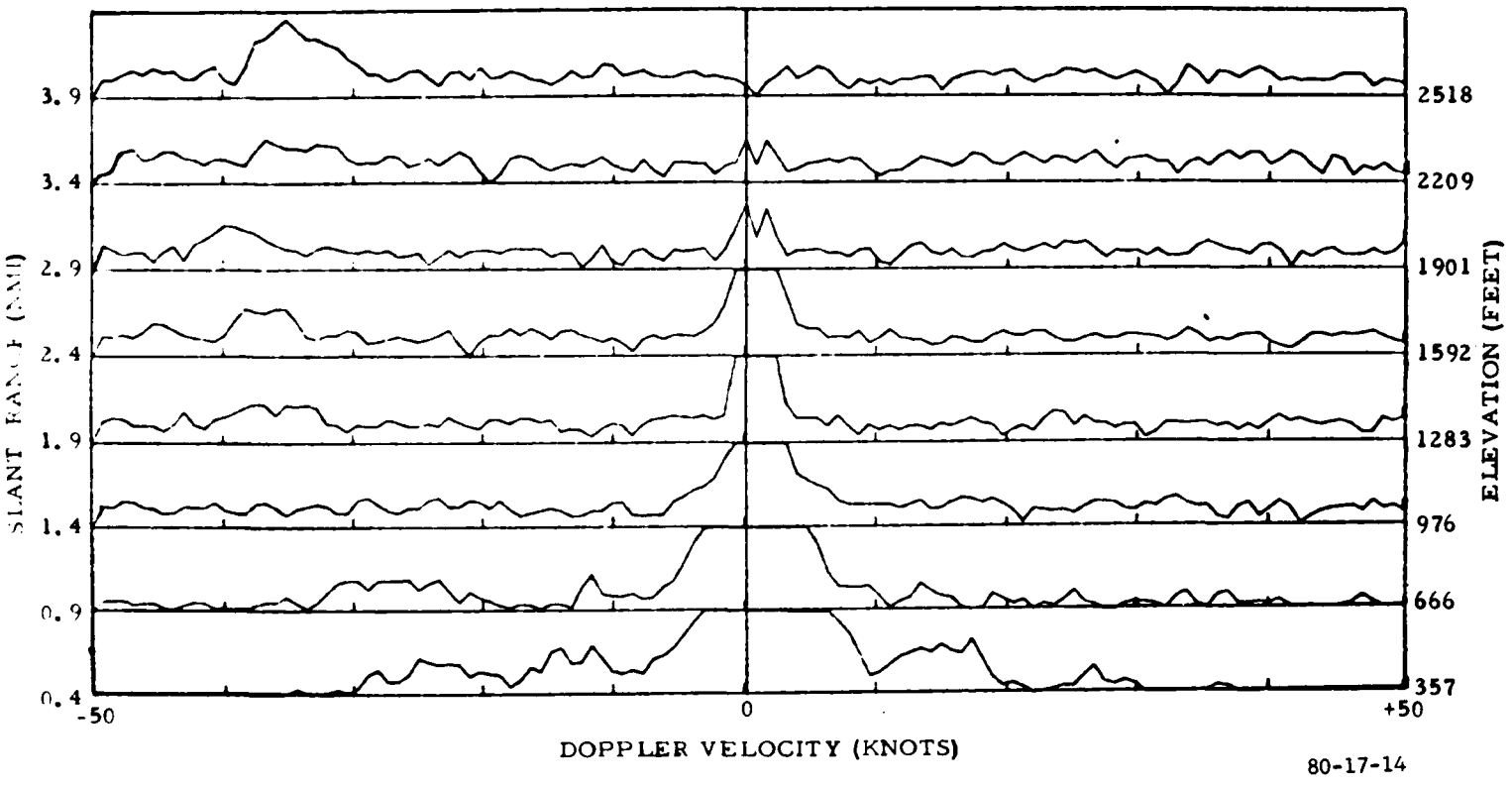

FIGURE 14. CLEAR AIR SPECTRA AT 6-DEGREE ELEVATION ANGLE

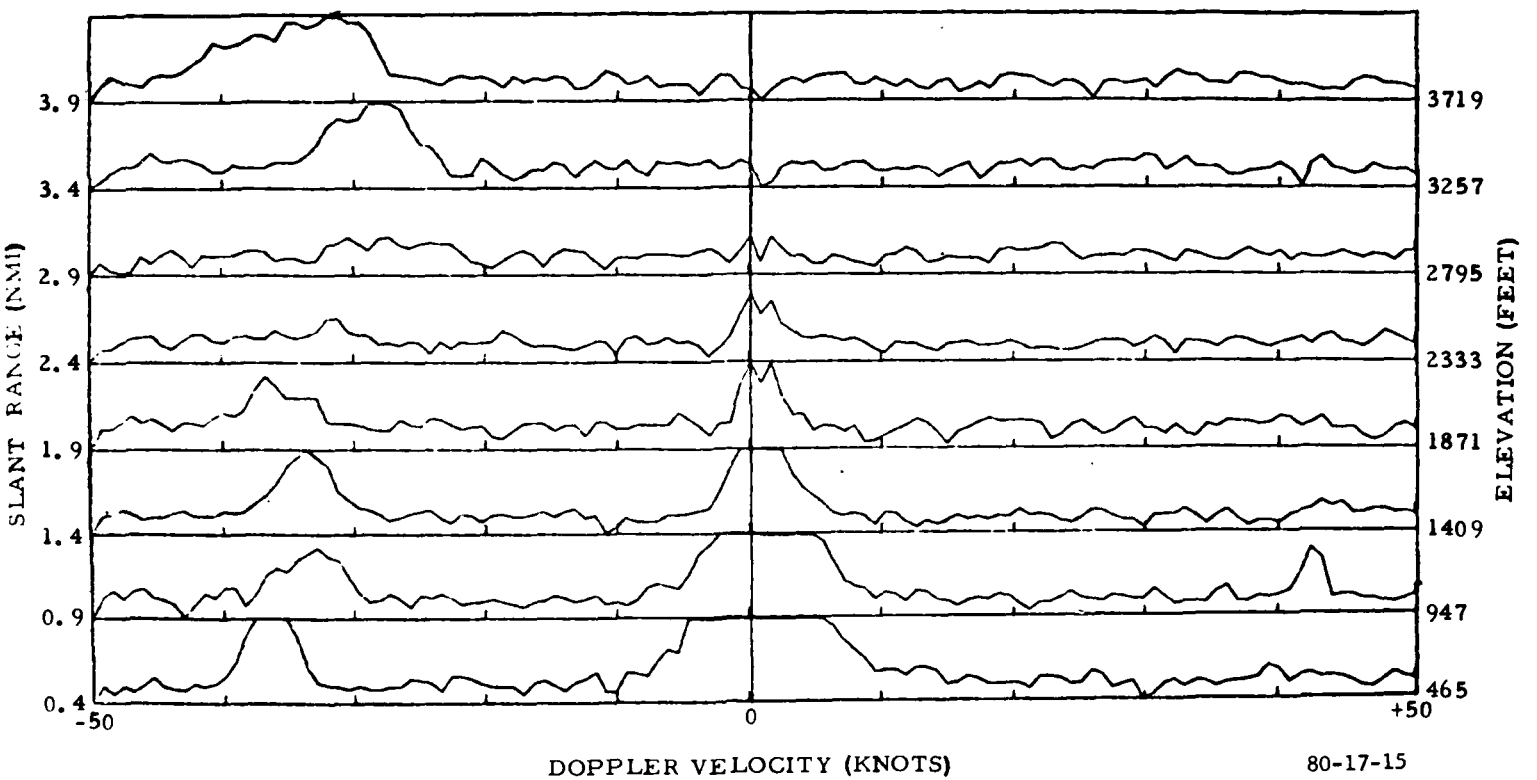

FIGURE 15. CLEAR AIR SPECTRA AT 9-DEGREE ELEVATION ANGLE

components measured by actual runway-oriented flights to within a one sigma accuracy of 3 to 7 knots.

4. A comparison of radar and tower winds showed agreement to within a one sigma directional accuracy of 11.5° to 14.7°, and a one sigma speed accuracy of 1.8 to 6.9 knots for the weather regimes encountered when the radar used a two-azimuth pointing technique.

5. Potentially dangerous radial wind shears associated with the weather encountered during these tests were detectable, but further investigation is required to determine operational applications.

6. System limitations may be resolvable through redesign and/or performance trade-offs.

RECOMMENDATIONS

It is recommended that tests be continued to:

1. Complete the definition of and demonstrate system capabilities in all weather situations (e.g., gust fronts associated with thunderstorms).

2. Optimize performance through redesign and/or trade-offs as necessary.

3. Provide information required to specify system design for possible development of prototype model.

REFERENCES

1. Offi, D. L. and Lewis, W., Preliminary Tests of the ASR-8 Wind Shear Detection System, Federal Aviation Administration, National Aviation Facilities Experimental Center, NAFEC Technical Letter Report No. NA-78-59-LR, December 1978.

2. Strauch, R. G., Monthly Progress Letter No. 26 Interagency Agreement, Department of Transportation, WPL, ERL, NOAA, Boulder, Colorado, DOT-FA76WAI-622 Task VII, June 1979.

3. Browning, K. A. and Wexler, R., The Determination of Kinematic Properties of a Wind Field Using Doppler Radar, Journal Applied Meteorology, 7, 105-113, 1968.

4. Strauch, R. G. and Sweezy, W. B., Wind Shear Detection with Pulse Doppler Radar, Federal Aviation Administration/SRDS, Washington, D.C., Final Report No. FAA-RD-80-26, January 1980.

5. Goldman, I., Power Density Measurements; Wind Shear/Turbulence Antenna, Federal Aviation Administration/ARD-243 Letter to File, July 1978.

6. Doviak, R. J., Zrnic, D. S., and Sirmans, D. S., Doppler Weather Radar, Proc. IEEE, Vol. 67, No. 11, pp 1522-1553, November 1979.

7. Sweezy, W. B., Moninger, W. R., and Strauch, R. G., Simulation of Radar-Measured Doppler Velocity Profiles in Low-Level Wind Shear (Phase 1), Federal Aviation Administration/SRDS Washington, D.C., Final Report No. FAA-RD-78-46, February 1978.

8. Chadwick, R. B., Moran, K. P., Morrison, G. E., and Campbell, W. C., Measurements Showing the Feasibility For Radar Detection of Hazardous Wind Shear at Airports, Hanscomb Air Force Base, Massachusetts, Final Report, AFGL-TR-78-0160, June 1978

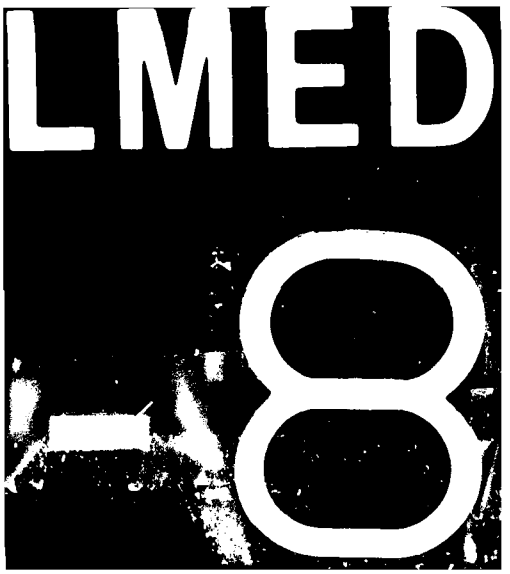
LMED
8